International Journal of Automotive Technology, Vol. 8, No. 2, pp. 127–135 (2007)

1229-9138/2007/033-01

EXPERIMENTAL STUDY ON THE FLOW AND MIXTURE DISTIBUTION IN A VISUALIZATION ENGINE USING DIGITAL PARTICLE IMAGE VELOCIMETRY AND ENTROPY ANALYSIS

K. H. LEE and C. H. LEE*

Department of Mechanical Engineering, Hanyang University, Gyeonggi 425-791, Korea

(Received 30 November 2005; Revised 5 June 2006)

ABSTRACT–The objective of this study is to analyze the effect of velocity and vorticity on stratified mixture formation in the visualization engine. In order to investigate spray behavior, the spray velocity is obtained through the cross-correlation PIV method, a useful optical diagnostics technology and the vorticity calculated from the spray velocity component. These results elucidated the relationship between vorticity and entropy, which play an important role in the diffusion process for the early injection case and the stratification process for the late injection case. In addition, we quantified the homogeneous diffusion rate of spray using entropy analysis based on Boltzmann's statistical thermodynamics. Using these methods, we discovered that the homogeneous mixture distribution is more effective as a momentum dissipation of surrounding air than that of the spray concentration with a change in the injection timing. We found that the homogenous diffusion rate increased as the injection timing moved to the early intake stroke process, and BTDC 60° was the most efficient injection timing for the stratified mixture formation during the compression stroke.

KEY WORDS : DISI Engine, Stratificatied mixture formation, Entropy analysis, Digital particle image velocimetry (DPIV)

NOMENCLATURE

I	: the intensity of an individual pixel
M	: the number of meshs
S	: entropy
S_1	: entropy of homogeneous divergencse
u	: X-directional velocity
v	: Y-directional velocity
α	: a proportionality factor
κ	: boltzmann's constant
ω	: vorticity

SUBSCRIPTS

i	: ith state
z	: interrogation area
t	: total

1. INTRODUCTION

As the environmenttal problems caused by vehicle exhaust emissions become more severe, exhaust emission standards and fuel economy regulations become more stringent. For the gasoline engine, the emission of CO_2, which is one of the main causes of global warming, has become a severe problem as well as the emission of toxic gases such as CO, HC, and NOx. Recently, the GDI (gasoline direct injection) engine has been spotlighted as the next generation engine that can satisfy the SULEV (Super Ultra Low Emission Vehicle) regulations and reduce fuel consumption. Thus, studies of a high-pressure, vortex-type injector, one of the key parts in the development of the GDI engine, have been performed by many researchers (Takagi and Teruyuki, 1998; Zhao *et al.*, 1996; Zhao and Lai, 1997; Toshio and Kochiro, 2004).

Zhao *et al.* (1996) visualized the development process of the fuel spray of the GDI injector by using a 2-dimensional Mie scattering method, and measured the SMD and the velocity of spray to investigate the evaporation of fuel. Many studies have investigated (Michael and Brad, 1998; Iwakiri and Kakuho, 1999) the characteristics of fuel injector spray, but because of experimental difficulties, detailed information on spray structure and the characteristics of the GDI injector are limited.

Yamakawa *et al.* (2001) developed a new fuel spray measuring technology known as LIF-PIV to measure the velocity of fuel spray with the ambient pressure. They investigated particle diameter, velocity distribution, and the evaporation process of the spray. Yuyama *et al.* (2001) developed a new entropy analysis method that is

*Corresponding author. e-mail: leemech@hanyang.ac.kr

based on statistical thermodynamics, and applied this method to the investigation of the propagation process of diesel spray. However, these previous studies indicated that there is still much uncertainty about the mixing process of gasoline direct injection. From this point of view, a more exact investigation of the mixture formation and the correlation between spray and induced air is required.

The paper begins with a brief description of the research engine and optical diagnostics used for the experiment. In this paper, firstly, the principle of the PIV, Vorticity and entropy analysis is briefly described, followed by the optical measurement system setup and experimental conditions. Finally, the effects of the spray velocity and vorticity with various injection timing in visualization engine and the stratification degree near the spark plug using entropy analysis are also described.

2. EXPERIMENTAL SETUP AND METHODS

2.1. Experimental Setup and Proceedings

Figure 1 shows the visualization system used to obtain the mixture distribution in the cylinder for simulating intake stroke in accordance with the changing intake flow field. A Nd:YAG laser (Contiuum Surelite I-10) was used as a light source, and the maximum power and wavelength was 200 mJ and 532 nm, respectively. The thickness of the induced-laser sheet beam was 500 um. The exposure time of the CCD camera, the illumination time of the laser beam, and the injection time of the fuel spray were controlled by a timing board (PC-TIO-10) and the Lab View program. The specifications of the visualization engine and injector are shown in Table 1 and Table 2.

Figure 2 shows the schematic diagram of the injector attached angle and optical window. The cylinder liner and piston are manufactured by quartz. The fuel spray

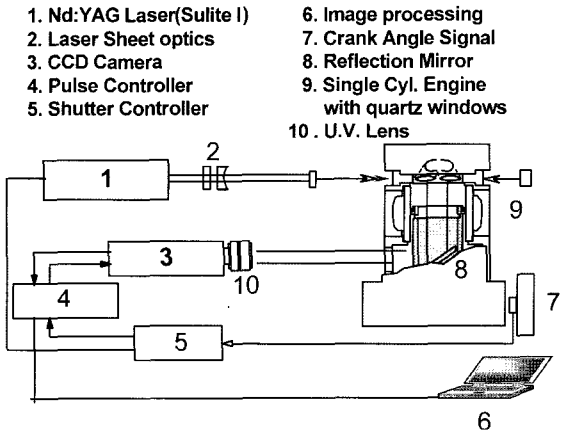

Figure 1. Schematics diagram of optical visual engine system.

Table 1. Specification of engine.

Item	Specification
Engine	DOHC single cylinder
Fuel	Gasoline
Clearance volume	47.3 cc
Bore×Stroke	81 mm×88 mm
Compression ratio	10.3
Operation speed	600 rpm

Table 2. Specification of GDI injectors.

Factor injector	Injection pressure	Spray pattern	Offset angle	Swirl
M	5MPa	Hollow cone	0°	o

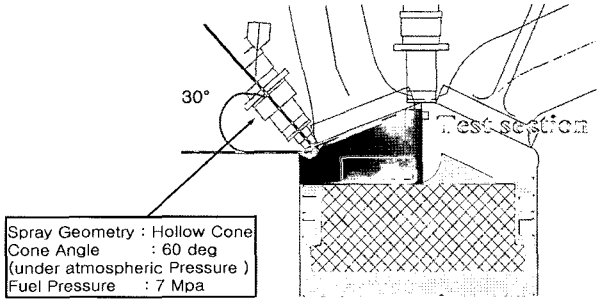

Figure 2. Configuration of test engine.

formation process and the mixture distribution in a single cylinder visualization engine were observed. The laser sheet beam was lighted into the in-cylinder through the cylinder liner and the transparent piston crown. To analyze the stratification effect near the spark plug at the late injection mode, the laser sheet beam was illuminated on a horizontal cross-section plane near the spark plug. Optical windows were installed at the top of the cylinder head gasket. The piston head was modified and transparent. The laser sheet beam was located 2 mm at the

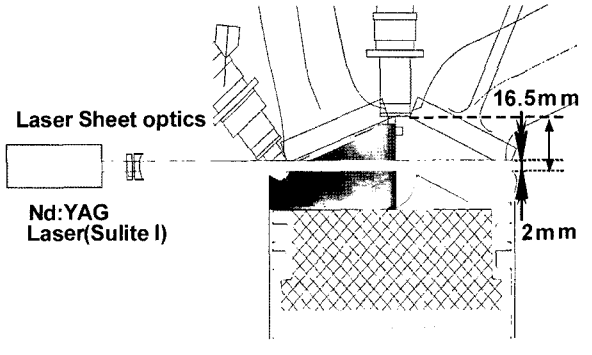

Figure 3. Schematic diagram of visualization region at compression stroke.

bottom of spark plug as shown in Figure 3. Using this system, we analyzed the fuel stratification characteristic near the spark plug in accordance with variable injection timing as the ignition timing is BTDC 20°.

2.2. Analysis Method

2.2.1. Cross-correlation particle image velocimetry

This section gives a brief description of the schematic diagram of frame straddling technique (Figure 4) and algorithm of the DPIV (Figure 5). The present study recorded particle images exposed by each sequential laser beam at separate frames by using a CCD camera and calculated the velocity vector by a cross-correlation PIV algorithm. The direction of particle velocity vector could be determined clearly because the particle images of each laser pulse were recorded at the separate frames. Figure 4 shows the 'frame-straddling' technique, which aligns the laser pulse at each sequential CCD camera frame. Laser pulse duation and exposure time are respectively 80 usec and 10 msec. Figure 5 shows the cross-correlation PIV algorithm using fast Furier transform (FFT), which is programmed to obtain the velocity by calculating the coordinates of location of the maximum cross-correlation parameter.

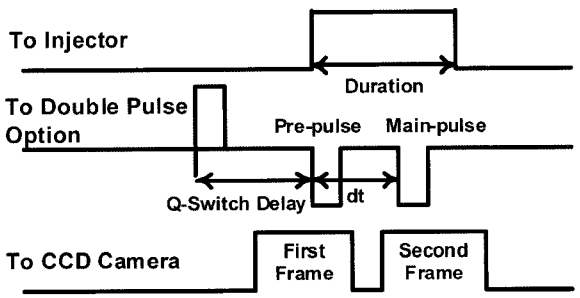

Figure 4. Schematic diagram of frame straddling and timing chart.

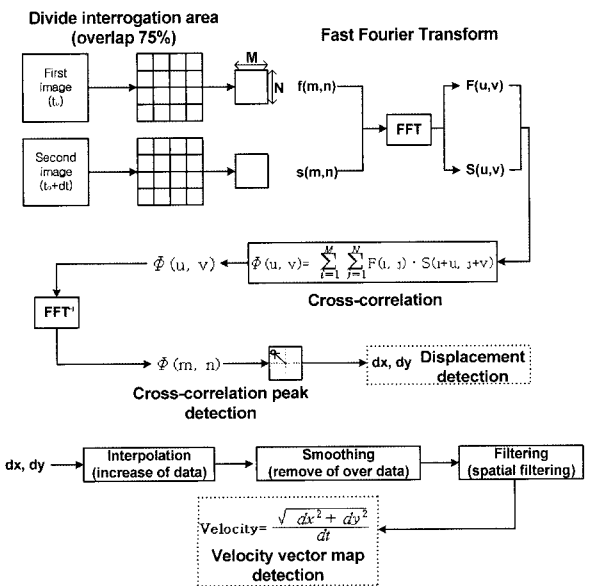

Figure 5. Schematic diagram of cross-correlation PIV algorithm.

2.2.2. Principle of vorticity measurement

In this study, we used the Ossen vortex algorithm (Luff (1999). Using the synthetic u and v velocity arrays derived from the Ossen expression, the synthetic vorticity array was generated numerically. Two prevailing techniques were evaluated. First, synthetic vorticity was calculated using a simple difference equation, which is the standard vorticity algorithm in NASA's plot 3-D software, as well as TSI's post-processing software. The data show:

$$\omega_5 \cong \frac{1}{\Delta L}\left[\frac{u_4 - u_6}{2} + \frac{u_2 - u_8}{2}\right] \tag{1}$$

Second, numerical vorticity was calculated using an 8-point circulation vorticity equation taken from Reuss *et al.*

$$\omega_5 = \frac{\Delta L}{(2\Delta L)^2}\left[\begin{array}{c}(u_2 - u_8) + (u_6 - u_4) \\ +0.5\left(\begin{array}{c}(u_3 - u_9) + (u_1 - u_7) \\ +(u_9 - u_7) + (u_3 - u_1)\end{array}\right)\end{array}\right] \tag{2}$$

Finally, most textbooks on numerical methods point out that higher order techniques provide higher accuracy because the order of approximation is improved. This does not necessarily hold true for noisy data, however, and so we have tested on the second order, the central difference approximation given by ref (Chapra, 1998) in order to ascertain how our techniques affect the estimator given here:

$$\omega_{13} = \frac{1}{\Delta L}\left[\begin{array}{c}\dfrac{(v_{11} - v_{15}) + (u_3 - u_{23})}{12} \\ +\dfrac{8(v_{14} - v_{12}) + 8(u_{18} - u_8)}{12}\end{array}\right] \tag{3}$$

This is one of several second order approaches one could adopt. A central difference scheme is the most appropriate for comparison to the other first order estimators.

In wat follows, the vorticity is calculated from the exact velocity, and velocity datea extracted by PIV respectively. From the reference (Ruan and Song, 2001; Luff, 1999) the second order central difference is quite appropriate to be used to extract the vorticity field from the velocity with higher uncertainty.

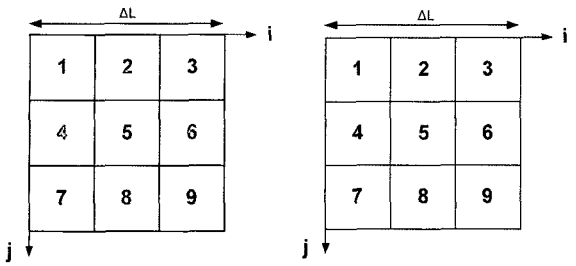

(a) Simple difference (b) 8-point circulation

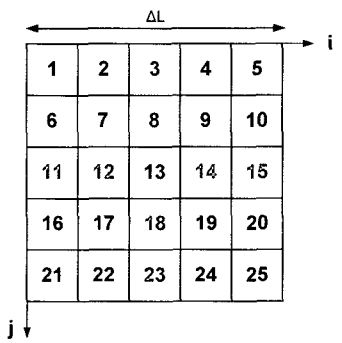

(c) Second order central difference

Figure 6. Schematic of sampling by the vorticity estimator presented in Equations (3), (4) and (5) (Luff *et al.*, 1999).

2.2.3. Entropy analysis

The entropy analysis of the laser scattering image is based on the concept of statistical thermodynamics. Boltzmann studied a correlation of the probability of particle distribution in the control volume and the entropy (Yuyama *et al.*, 2000).

Using the entroy analysis the entropy of a homogeneous divergence (S_1) is then:

$$S_1 = \alpha \cdot I_t \cdot \ln(M) \tag{4}$$

M is the number of cells in an image, and α is a constant including a Boltzmann constant and the proportional coefficient between the number of particles and the image intensity. I_t is the integrated value of the image intensity over the whole image area.

The image intensity is divided into 0 and 255 with the total image intensity kept constant. So the entropy obtained by the divided image intensity is calculated as

$$S_0 = \alpha \cdot [I_t \ln(I_t) - I_t \cdot \ln(I_{MAX})] \tag{5}$$

Where P is the number of cells that fluorescent light 255 occupy.

The normalized entropy S^* can be defined as

$$S^* = \frac{S - S_0}{S_1 - S_0} = \frac{I_t \ln(I_{MAX}) - \sum_i^M \{I_{(i)} \cdot \ln(I_{(i)})\}}{I_t \cdot \{\ln(M) - \ln(I_t) + \ln(I_{MAX})\}} \tag{6}$$

The homogeneity and heterogeneousity degree of the spray and the diffusion phenomena can be analyzed by normalized entropy.

3. RESULTS AND DISCUSSIONS

3.1. Flow Velocity and Vorticity Distribution in the Cylinder

Figure 7 shows the results obtained for the flow velocity in the cylinder in accordance with changing the crank angle or valve lift for the intake stroke as the number of rotations is 600 (rpm). We calculated the flow velocity from ATDC 90° to ATDC 150° by 20° CA. As shown in Figure 7, we know that the maximum intake flow rate is 130° CA. From the results, the flow entered intake port separates toward both walls and in the cylinder occurs at the reverse tumble flow. The reason for this is the performance of the intake port. The velocity of the left side is strong but that of the right side is diminished. In the case of the commercial port, that of the right side is strong. Accordingly, as the crank angle increases, the velocity of the left side is active; then after ATDC 150°, it is inactive. But the velocity of the right side diminishes gradually in accordance with the increasing crank angle. Figure 7 shows the results of vorticity in accordance with the increasing crank angle using the algorithm of the Ossen vortex as seen in Figure 6. The strongest part of the vorticity is the middle in the cylinder and then, as the crank angle is increased, the vorticity gradually decreases. We observed that the reverse collision tumble flow slightly decreased and then formed a vortex. As the crank angle increased, the vortex forming the interactive collision gradually decreased. As shown in Figure 8, we found that the maximum average velocity in cylinder flow is 9 m/sec, at 110° ATDC; as the crank angle increases, the velocity gradually decreases.

3.2. Spray Velocity to the Free Spray

Figure 9 shows the velocity distribution of the vertical tomogram of the spray at 2 msec and 3 msec from the ignition of the injection at an ambient pressure of 0.1 MPa. The leading edge and central part of the spray shows relatively high velocity. Especially, although the velocity scale is small, a clear counter-rotating vortex motion is observed on the periphery of the spray. In particular, by carefully investigating the direction and scale of the velocity vectors in the spray periphery, the velocity vectors were found to indicate directly the negative axial direction in the axial distance of 20~30 mm with a small vortex scale in the case of the injection duration of 2 msec and 30~50 mm with a large vortex scale in the case of the injection duration of 4 msec.

Figure 10 shows the maximum velocity in accordance with injection duration such as 2 msec, 3 msec, and 4 msec. As the injection duration is increased, the maximum

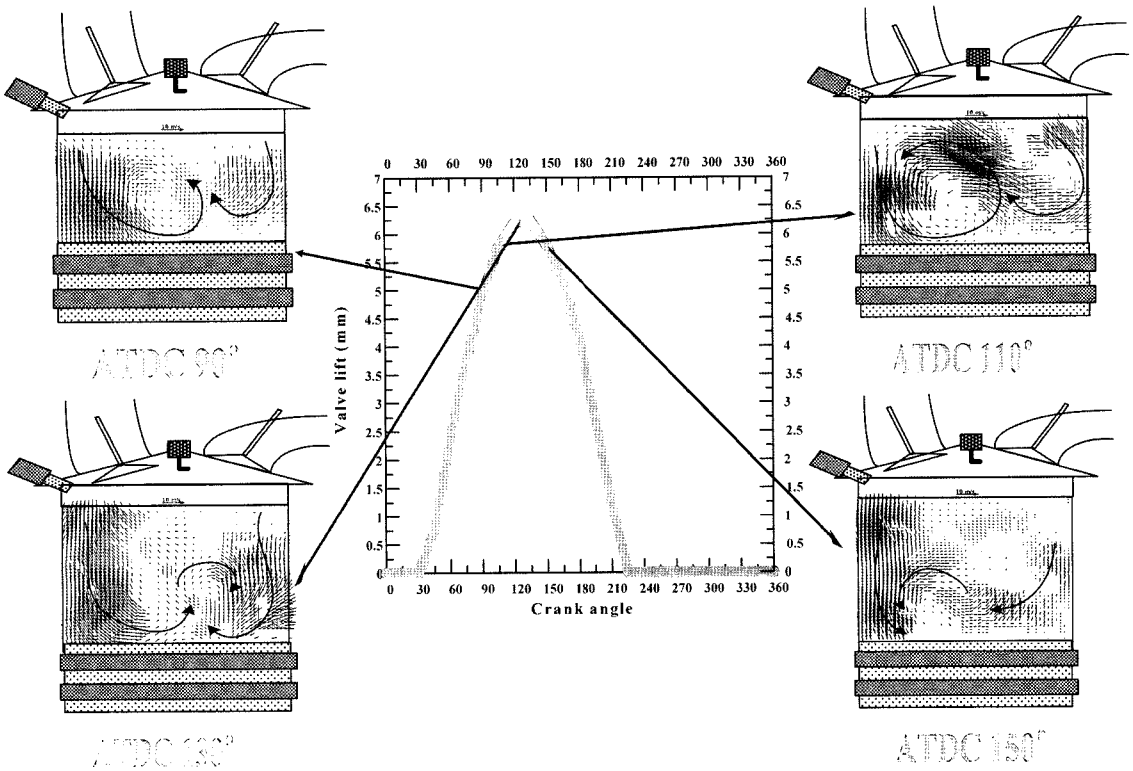

Figure 7. The velocity and vorticity distribution in accordance with crank angle at intake stroke.

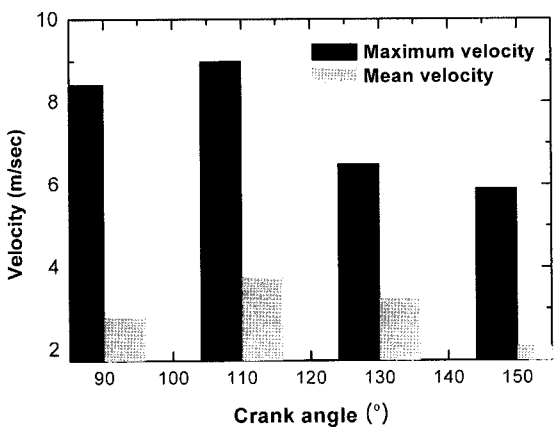

Figure 8. Average velocity according to crank angle.

velocity after the end of the injection in accordance with the elapsing time is increased. The maximum velocity in injection duration is 10 m/sec, at 2 msec, 12 m/sec, at 3 msec, and 15 m/sec, at 4 msec, respectively.

3.3. Spray Velocity and Vorticity in the Cylinder

Figure 11 shows the velocity and vorticity distribution of spray droplet in accordance with injection timing using the cross-correlation PIV technique and second order central difference method of the Ossen vorticity algorithm. Generally vortex is shown in the left and right but the vortex on the right side is not observed in this result due to the intake flow. From Figure 8, as the velocity is high in case of 90~110° ATDC the location of the generated vortex moves to the middle direction of in-cylinder and disturbs the spray velocity distribution. Also we found that the spray velocity is involved in the intake flow and the fuel spray is dispersed on the in-cylinder homogeneously. In particular, investigating carefully, we examined the direction and scale of velocity vectors and vorticity strength in the cylinder. We also can see that the velocity vectors indicate directly the negative axial direction in axial distance of 25~35 mm with ATDC 90~130° and about 20 mm with ATDC 150.

Figure 12 shows the vorticity of the elapsing timing after injection. As seen in Figure 11, when the injection time is at 110° ATDC, the vortex size is the largest. And in the case of 1.6 msec after the end of the injection (AEOI), the vorticity strength is highest at 110° ATDC. Finally, we found that this condition is optimized when involved in the intake flow and spray behavior of the visual engine.

3.4. Stratification Effect of Fuel using Entropy Analysis

Figure 13 shows the fuel stratification and mixture procedure using entropy analysis. We introduced entropy analysis of statistical thermodynamics to analyze quantitatively the diffusion of the mixture distribution and

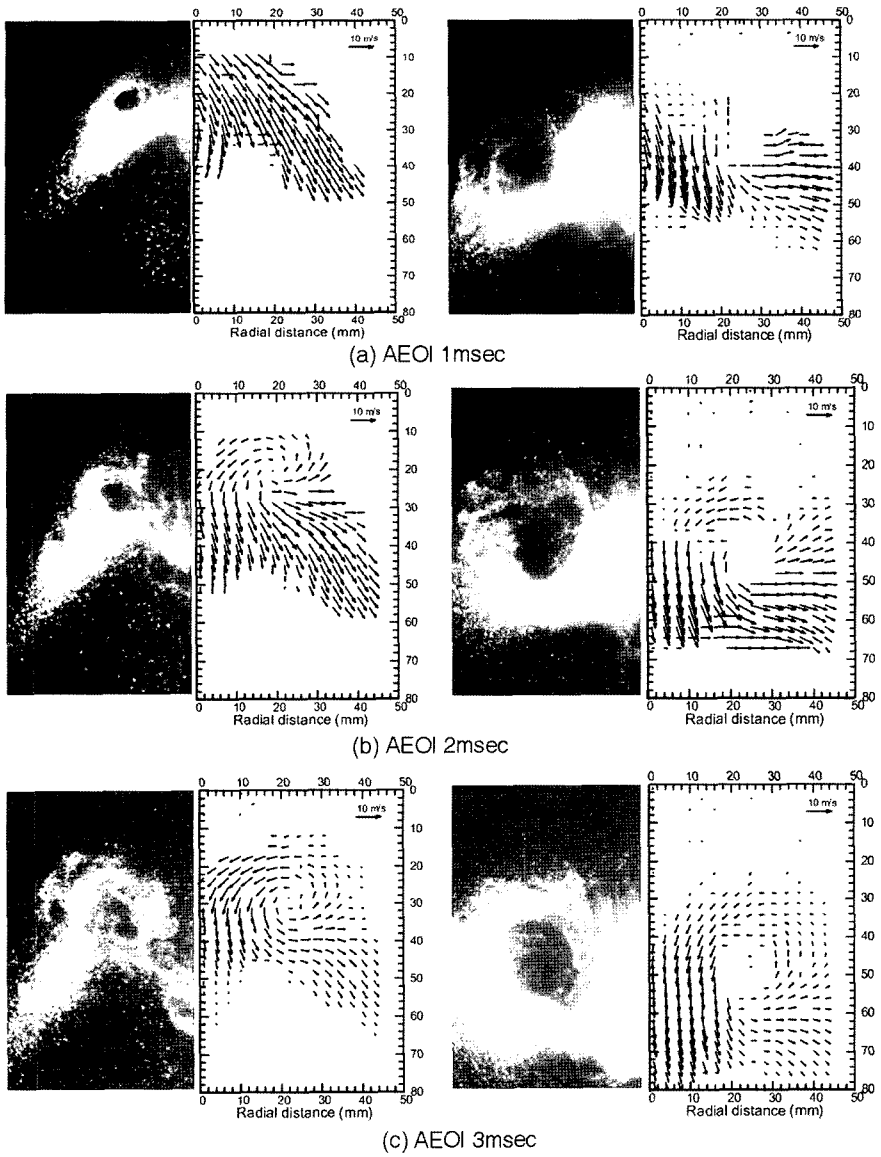

Figure 9. The spray developing process and spray velocity distribution in accordance with elapsing time to injection duration (left side: 2 msec at injection duration, right side: 4 msec at injection duration).

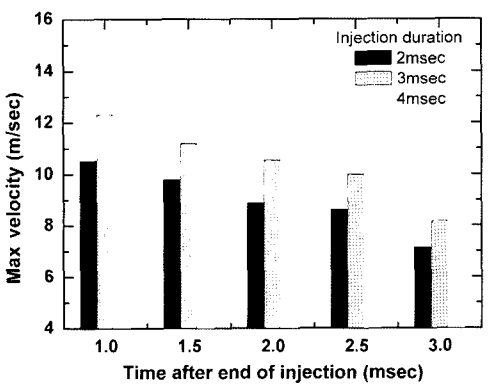

Figure 10. The maximum velocity with injection duration.

homogeneous degree (Yuyama *et al.*, 2000). This result shows the arrival of fuel at spark plug duting stratified operation (late injection mode). It present a sequence of average imagees between 20 cycles. We observed the stratification effects near the spark plug at the compression stroke and set the injection timing from 40° BTDC to 80° BTDC at 10° CA intervals. When the ignition timing was set to 20° BTDC, we observed stratification near the spark plug in accordance with the injection timing in the late mode. In the case of the injection timing at 50° BTDC and 60° BTDC, the stratification effect is higher than in other conditions. As the injection timing was slowed and speeded up, the stratified effect near the

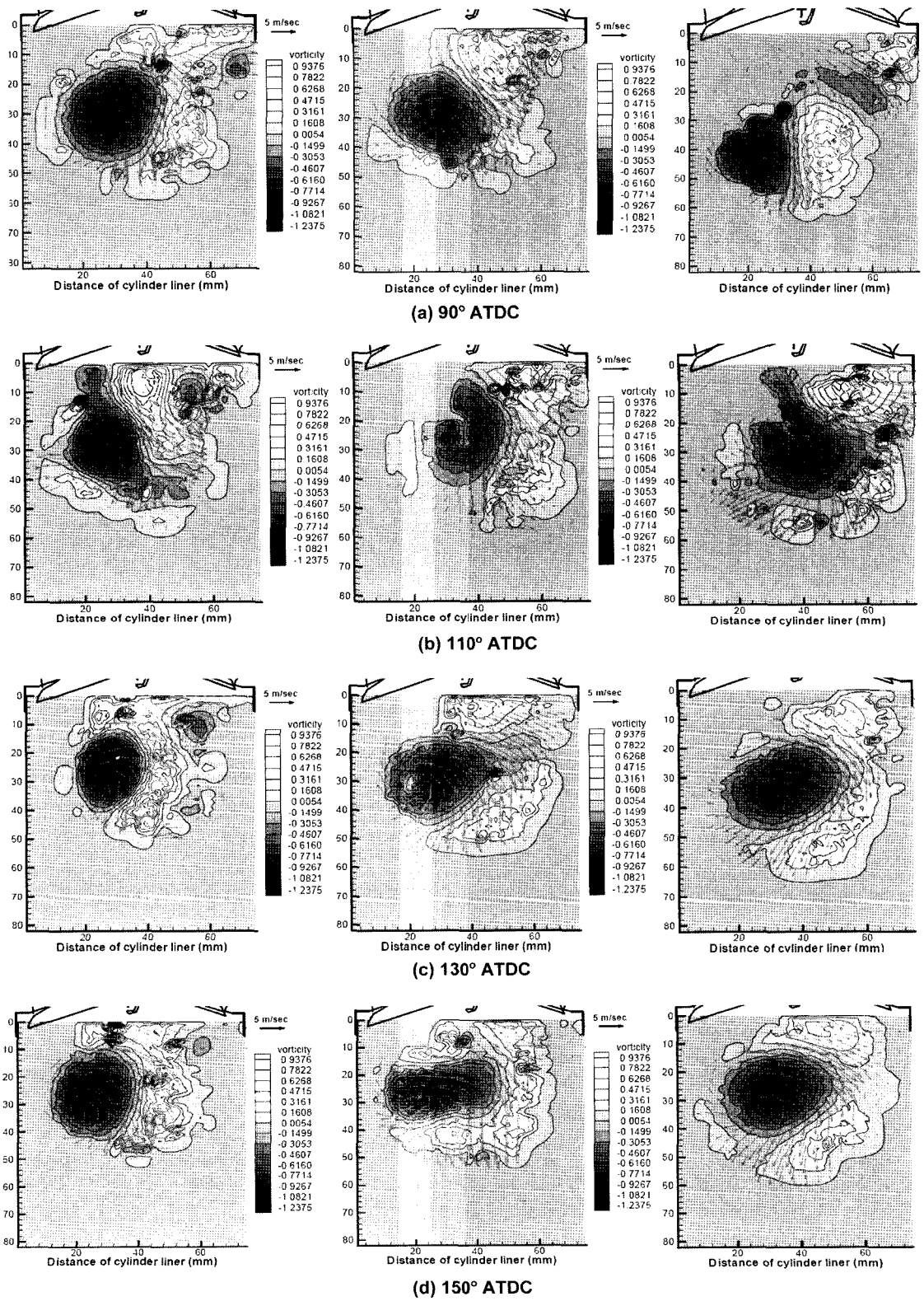

Figure 11. The spray velocity and vorticity in accordance with changing the injection timing.

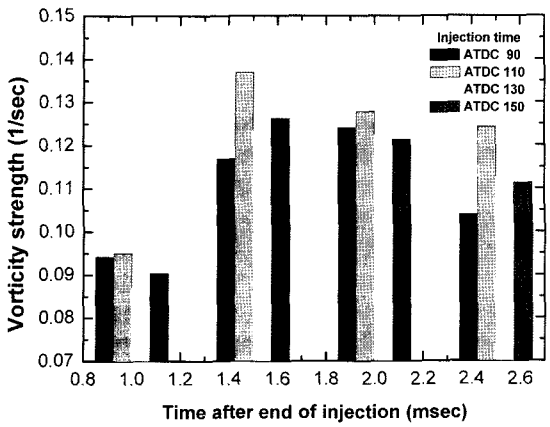

Figure 12. the average vorticity in accordance with changing the injection timing.

spark plug became less. The behavior of ignition in stratified mode are a function of injection timing. One part of the fuel is carried out directly form the injector to the spark plug with impinging the piston. From this result the important parameter is injection timing and ignition event. In case of stratified mode injection timing and ignition event timing are BTDC 60° and BTDC 20°.

4. CONCLUSIONS

A new entropy analysis method based on statistical thermodynamics and the cross-correlation PIV measurement method has been developed. In this study, we understood the optimal conditions and characteristics through analysis of the stratification effect and the velocity field measurement of the cylinder.

(1) Investigating carefully the direction and scale of velocity vectors in the spray periphery, we found that the velocity vectors indicate directly the negative axial direction in the axial distance of 20~30 mm with a small vortex scale in the case of an injection duration of 2 msec and 30~50 m with a large vortex scale in the case of an injection duration of 4 msec.

(2) We found that the maximum average velocity in the cylinder flow is 9 m/sec, at 110° ATDC, and when the crank angle is increased, the velocity gradually decreased.

(3) By using the Mie-scattering method, entropy analysis, and particle image velocimetry, through this method, we found that the spray velocity is involved in the intake flow and the fuel spray is dispersed on the in-cylinder homogeneously at an injection timing of 110° ATDC.

(4) We also found that the heterogeneous diffusion rate increased as the injection timing moved to the early intake stroke process, and BTDC 60° was the most efficient injection timing for the stratified mixture formation during the compression stroke.

(5) The analysis of stratification effect feature using the

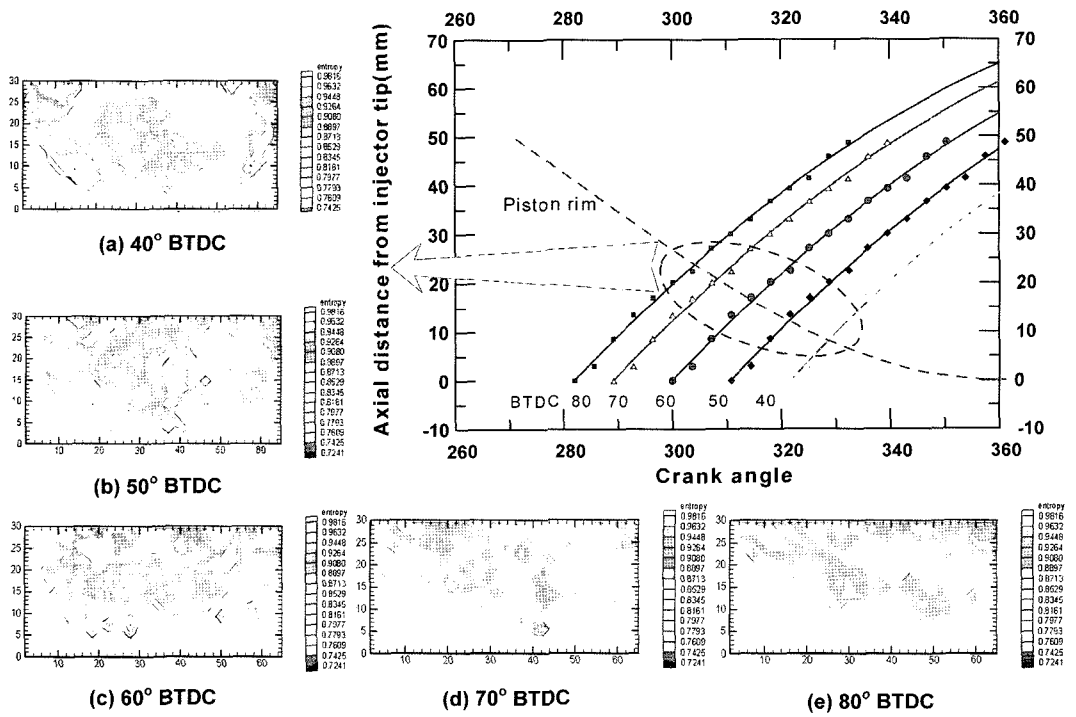

Figure 13. The stratified characteristics in accordance with injection timing at compression stroke using the entropy analysis.

entropy analysis enables to evaluate the mixture formation, which is stratification feature, in relation to an actual combustion system.

ACKNOWLEDGEMENT–This study was made possible with funding from the CERC (Combustion Engineering Research Center), and we would like to show appreciation to its associated organizations.

REFERENCES

Chapra, S. C. (1998). *Numerical Methods for Engineers.* McGraw-Hill Inc.. New York. 529.

Iwakiri, Y. and Kakuho, A. (1999). Effectiveness and issues of various measurement techniques used in evaluating spray characteristics in a direct-injection gasoline engine. *Pro. 15th Int. Com. Engine Symp.* 9935095.

Kume, T., Iwamoto, Y., Iida, K., Murakami, M. Akishino, K. and Ando, H. (1996). Combustion controlled technologies for direct injection SI engine. *SAE Paper No.* 960600.

Luff, J. D. (1999). Experimental uncertainties associated with particle image velocimetry based vorticity algorithms. *Exp. Fluids,* **26**, 36–54.

Michael, H. and Brad, A. (1998). Early spray development in gasoline direct-injected spark ignition engine. *SAE Paper No.* 980160.

Preussner, C. and Döring Fehier, S. and Kampmann, S. (1998). GDI: Interaction between mixture preparation, combustion system and injector performance. *SAE Paper No.* 980498.

Ruan, X. and Song, X. (2001). Direct measurement of the vorticity field in digital particle images. *Exp. Fluids,* **30**, 696–704.

Takagi, Y. and Teruyuki, T. (1998). Simultaneous attainment of low fuel consumption, high output power and low exhaust emissions in direct injection SI engine. *SAE Paper No.* 980149.

Toshio, S. and Koichiro, T. (2001). Analysis of direct injection SI stratified combustion in hydrogen lean mixture–combustion promotion and cooling loss. *Int. J. Automotive Technology* **2**, **3**, 85–91.

Yamakawa, M., Isshiki, S., Yoshizaki, T. and Nishida, K. (2001). Measurement of ambient air motion of D.I. gasoline spray by LIF-PIV. *COMODIA 2001*, 499–504.

Yuyama, R., Chikahisa, T., Kikuta, K. and Hishinuma, (2001). Entropy analysis of microscopic diffusion phenomena in diesel sprays. *COMODIA 2001*, 542-550.

Zhao, F. Q. and Lai, M. C. (1997). A review of mixture preparation and combustion control strategies for spark-ignited direct-Injection gasoline engine. *SAE Paper No.* 970627.

Zhao, F.-Q., Yoo, J.-H. and Lai, M.-C. (1996). Spray dynamics of high pressure fuel injectors for DI gasoline engines. *SAE Paper No.* 961925.